6

Ionic Polymer-Metal Composite as a New Actuator and Transducer Material

K. J. Kim

Active Materials and Processing Laboratory, Mechanical Engineering Department (MS 312), University of Nevada, Reno, Nevada 89557, U.S.A.

6.1 Introduction

Ionic polymer-metal composites (IPMCs) are a unique polymer transducer that when subjected to an imposed bending stress exhibits a measurable charge across the chemically and/or physically placed effective electrodes of the electroactive polymer. IPMCs are also known as bending actuators capable of large bending motion when subjected to a low applied electric field (~10 kV/m) across the metalized or conductive surface (Figure 6.1). The voltage found across the IPMC under an imposed bending stress is one to two orders of magnitude smaller than the voltage required to replicate the bending motion input into the system. This leads to the observation that the material is quite attractive by showing inclination for possible transduction as well as actuation [1–25]. In 1993, an IPMC was first reported as an active polymeric material by Oguro and his co-workers [21]. Since then, much attention has been given to IPMCs with the hope that they can be used as a soft actuator and sensor/transducer material for new opportunities in future engineering. IPMCs have been considered promising actuator materials, in particular for biorobotic applications.

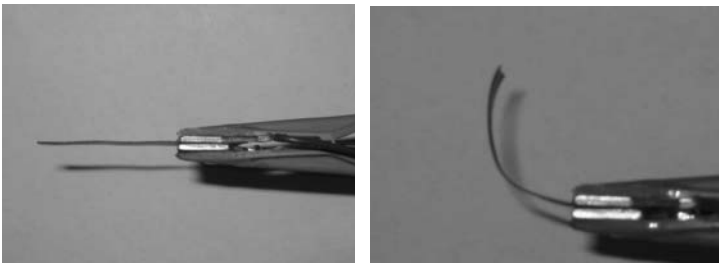

Figure 6.1. Actuation of a typical IPMC (from [8])

Part of what makes an IPMC so unique are its inherent transductive/sensing properties in addition to its actuation capabilities. Similar to piezo materials, IPMCs can show displacements under an applied electric field and can also

engender a current from an imposed bending moment that is applied to the material. The voltage can be as high as in the 10's of millivolts range for larger imposed bending displacements. This makes IPMCs possibly effective for large motion sensor or damper applications if their behavior can be properly controlled.

6.2 How IPMC Works

In 2000, De Gennes *et al*. [18] presented a set of coupled equations based on linear irreversible thermodynamics to describe the behavior of a typical IPMC. The model is a compact description of the transduction and actuation principles inherent in the IPMC by defining it in the linear regime and in static conditions.

They introduce the linear irreversible thermodynamic relationship for charge transport (with a current density J normal to the membrane) and solvent transport (with a flux Q) to describe this electromechanical coupling of ionic gels (*i.e*. IPMCs, see Figure 6.2 [18]). The standard Onsager relations for the system have the form,

$$J = \sigma E - L_{12}\nabla p \tag{6.1}$$

$$Q = L_{21}E - K\nabla p \tag{6.2}$$

Equations (6.1) and (6.2) couple the electric field, E, as well as the mechanical pressure gradient, ∇p, the driving forces for the phenomenon involved. These equations can be elaborated upon to explain the direct effect (actuation) as well as the inverse effect (sensing or transduction) of IPMCs. Note that these Onsager relations developed by De Gennes *et al*. are for a static model. Note also that σ, L_{12} (=L_{21}), and K are electric conductance, cross-coefficient, and permeability, respectively.

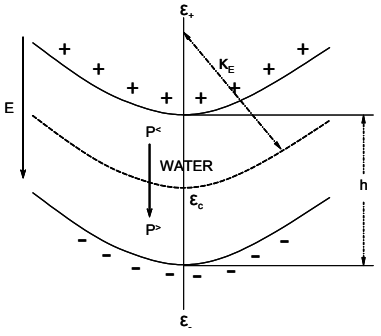

Figure 6.2. Principle of the bending motion. K_E, h, E, and P are the curvature, specimen thickness, electric field, and ionic pressure of the system.

IPMCs as transducers have been modeled and developed for actuation, sensing. and control applications by several investigators. Their work can be found elsewhere [19–25].

6.3 IPMC Manufacturing Techniques

6.3.1 Metal Reduction Technique

The current state-of-the-art IPMC manufacturing technique [6] incorporates two distinct preparation processes: *initial compositing process* and *surface electroding process*. Due to different preparation processes, the morphologies of precipitated platinum are significantly different. The initial compositing process requires an appropriate platinum salt such as $Pt(NH_3)_4HCl$ for chemical reduction processes. The principle of the compositing process is to metalize the inner surface of the material (usually, Pt nano–particles, in a membrane shape) by a chemical-reduction means such as $LiBH_4$ or $NaBH_4$. The ion-exchange polymer is soaked in a salt solution to allow platinum-containing cations to diffuse through *via* the ion-exchange process. Later, a proper reducing agent such as $LiBH_4$ or $NaBH_4$ is introduced to platinize the materials by molecular plating. It has been experimentally observed that the platinum particulate layer is buried a few microns deep (typically 1–10 μm) within the IPMC surface and is highly dispersed. A TEM image near the boundary region of an IPMC strip on the penetrating edge of the IPMC shows a functional particle density gradient where the higher particle density is toward the surface electrode. Figure 6.3 describes Ni-doped IPMC manufacturing developed at the Active Materials and Processing Laboratory of the University of Nevada, Reno.

6.3.2 Physical Loading Technique

Although the traditional metal reduction processes described above are known to be effective in manufacturing IPMCs, one may realize that one drawback of using these processes is their relatively high cost due to the use of noble metals (platinum, gold, palladium, *etc*.) and associated complex chemical processes. For IPMCs to be successfully adopted as industrial actuators or sensors, one should be able to reduce their manufacturing cost significantly. One way to do so is to simplify the compositing and electroding processes.

The principal idea of processing this new IPMCs is first to physically load a conductive primary powder into the polymer network forming a dispersed layer which can function as a major conductive medium near boundaries and, subsequently, to further secure such a primary particulate medium within the polymer network with smaller particles (Pd or Pt in this case) via a chemical plating process so that both primary and smaller secondary particles can be secured within the polymer network. Furthermore, an electroplating process can be applied to integrate the entire conductive phase intact, serving as an effective electrode. For more details, readers are referred to recent work done by Shahinpoor and Kim [15].

This physical loading technique has been elaborated by Leo and his co-workers [25]. They used a high surface area-to-volume ratio of metal particulates to achieve high capacitance at low frequencies.

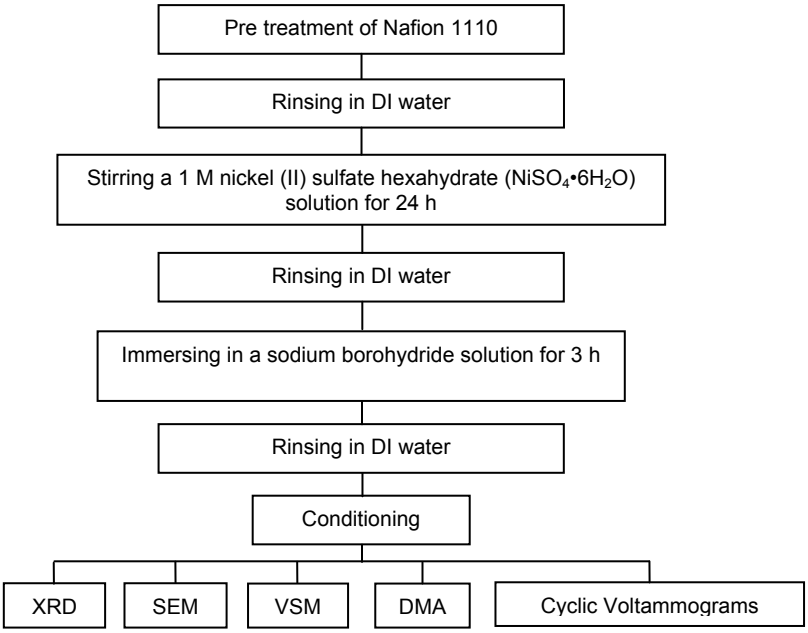

Figure 6.3. Experimental procedure for Ni-doped IPMCs using the ion-exchange and precipitation method

6.4 Engineering Properties of Interest

In this section, important engineering properterties of typical IPMCs are presented.

6.4.1 Mechanical Properties

Figure 6.4 shows the results of dynamic material analysis (DMA) tests for a pristine Nafion^{TM} film and a Ni-doped IPMC in tensile. The experiment was performed in air. In the tensile mode, Ni-doped IPMCs have higher storage modulus (E') with regard to stiffness than pristine Nafion^{TM} film.

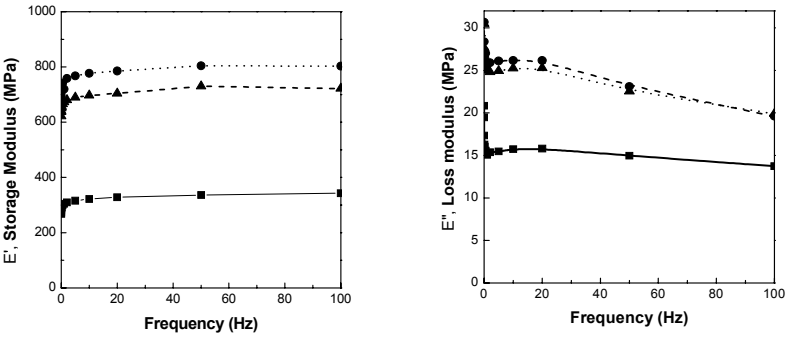

Figure 6.4. DMA results of the pristine Nafion film (■) and metal-doped IPMCs (● and ▲). The results are storage modulus (a) and loss modulus (b) with a frequency range from 0.01 to 100 Hz in the tensile mode

6.4.2. Electrical and Electrochemical Properties

6.4.2.1 General Electrical Properties

To assess the electrical properties of an IPMC, the standard AC impedance method that can reveal the equivalent electric circuit has been adopted. A typical measured impedance plot, provided in Figure 6.5, shows the frequency dependency of the impedance of the IPMC. It is interesting to note that the IPMC is nearly resistive in the high–frequency range and fairly capacitive in the low–frequency range.

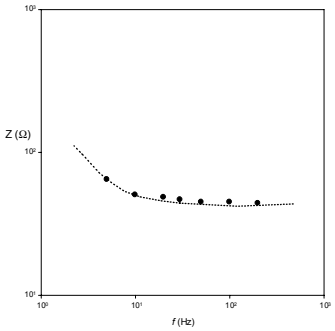

Figure 6.5. The measured AC impedance spectra (magnitude) of an IPMC sample [6]

Based upon the above findings, a simplified equivalent electric circuit of the typical IPMC can be considered, such as the one shown in Figure 6.6. In this approach, each single unit-circuit (i) is assumed to be connected in a series of arbitrary surface-resistance (R_{ss}) in the surface. This approach is based upon the experimental observation of the considerable surface-electrode resistance. We assume that there are four components to each single unit-circuit: the surface-electrode resistance (R_s), the polymer resistance (R_p), the capacitance related to the ionic polymer and the double layer at the surface-electrode/electrolyte interface (C_d), and an impedance (Z_w) due to charge transfer resistance near the surface

electrode. For the typical IPMC, the importance of R_{ss} relative to R_s may be interpreted from $\Sigma R_{ss} / R_s \approx L / t >> 1$, where notations L and t are the length and thickness of the electrode, respectively.

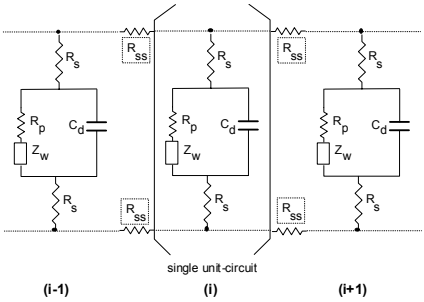

Figure 6.6. A possible equivalent electric circuit of a typical IPMC membrane [6]

6.4.2.2 Electrochemical Properties

Figure 6.7 shows cyclic voltammograms of an IPMC with platinum electrodes. Potentiostat/galvanostat (PGZ40, Voltalab) was used for the cyclic voltammetry as well as AC impedance. By examining the voltammogram of the IPMC, it is clear to see the polycrystalline characteristics of the platinum that has been significantly altered by the presence of the base polymeric material within the testing specimen showing a unique behavior. This exhibits the importance of the surface properties of the electrodes of an IPMC. The electrochemical behavior at the surface electrodes is yet to be determined and is currently under investigation.

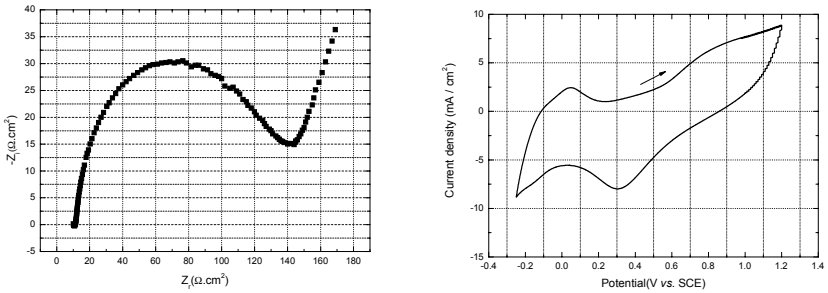

(a) (b)

Figure 6.7. Electrochemical impedance behavior (a) and cyclic voltammograms (b) with a scan rate of 50 mV/s in 0.5M sulfuric acid of an IPMC [5]

6.4.2.3 Measurement of the Force-displacement Relationship

The electromechanical properties considered are determined by the force–displacement relationship of an IPMC actuator. The method used to measure these properties is graphically depicted in Figure 6.8. An IPMC actuator is cantilevered at one end, and the other end is constrained, as shown in Figure 6.8a. The reaction force (or actuation force) at the right end of the actuator is generated by an

electrical field. We measure the reaction force with a small force transducer. After the right-end constraint is moved up with amount of the displacement s, the same test is conducted. In this way, the actuation force corresponding to the end displacement s can be measured, as illustrated in Figure 6.8b. Finally, without the constraint, the free end displacement can be determined. Following this procedure, the force-displacement relationship was obtained as shown in Figure 6.9. Figure 6.9 shows the measured force-displacement relationship for an IPMC actuator for two- and three-volt inputs across the IPMC. Regions **A** and **B** in Figure 6.9 include the maximum actuation forces and the maximum displacements, respectively. The specimen tested was a Nafion^{TM}-based IPMC in Li^+ form and plated with platinum. The length of the IPMC actuator was 20 mm with a width of 5 mm and a thickness of 0.3 mm.

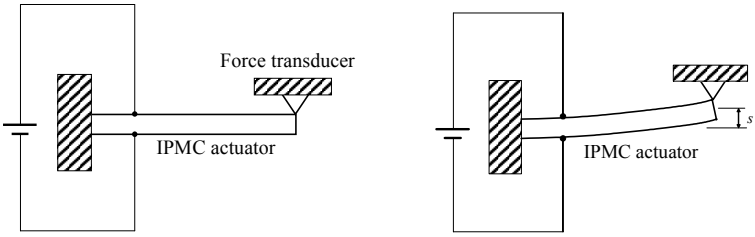

Figure 6.8. Test setup for the force-displacement relationship ([4])

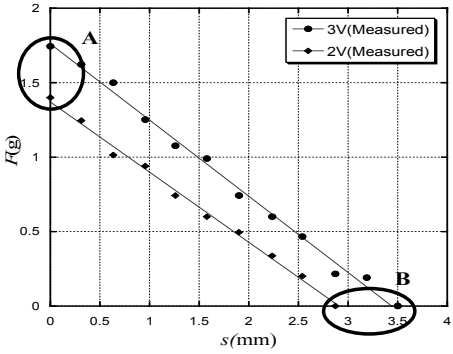

Figure 6.9. Force-displacement relationship of an IPMC actuator ([4])

Thus, the force F for $s = 0$ (region **A** in Figure 6.9) is the reaction force for the case shown in Figure 6.8a, and the measured displacement s when $F = 0$ (region **B** in Figure 6.9) stands for the tip displacement without the right-end constraint.

6.5 Robotic Flapping Wings

Pneumatic and motor-driven actuators have been widely adopted and used in aerospace applications as well as in other industrial robot systems. However, these actuators are not feasible for use in small or microscale flying and locomotive vehicles due to their large payload and system complexity. Furthermore, they are not suitable for mimicking the flapping motion of bird or insect wings. Using microrobots to create flapping flight is attractive due to their maneuverability that could not be obtained by conventional, fixed or rotary wing aircraft. An electroactive polymer, IPMC is a good candidate for the flapping motor because it is lightweight and can create a large deformation under low electric voltage input. Bird/insect wings can generate lift and thrust at the same time during flapping motion because the wing can flap and twist during the flapping motion [26]. To mimic the motion, the artificial flapping mechanism should also be able to create flap and twist simultaneously. Also, the width of a bird wing tip is pointed compared with the remaining parts of the wing. This reduces drag during the up-/down-strokes of the wing and also strengthens the tip of the vortex. Thus, the actuation mechanism and shape are both important for successfully mimicking a bird wing. The IPMC can generate this particular motion if it has a specially designed plan form.

Since the flapping wing must create a twisting motion as well as a bending up and down motion for thrust generation, the IPMC actuators have nonsymmetric-shapes, as shown in the two wings in Figure 6.10. The wing shapes and dimensions of the wings are also shown in Figure 6.10. Note that the areas of the IPMC actuators in the two wings are kept the same for fair comparison in the actuation displacement analysis. The wing itself is made of a thin plastic film.

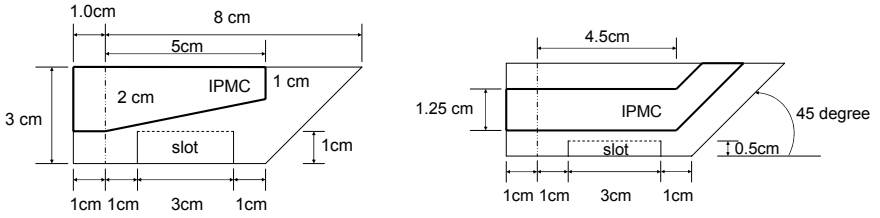

(a) Wing #1 (b) Wing #2

Figure 6.10. Flapping wing and patterns of IPMC actuators ([27])

The numerical deformation analysis has been conducted to determine the shape of the IPMC actuator such that the designed wing can produce maximum bending and twisting motion at the same time. Deformation of the wing has been estimated by using the equivalent bimorph beam model and MSC/ NASTRAN with the thermal analogy. For finite-element modeling, QUAD4 elements were used for both Wing #1 and #2 as shown in Figure 6.11a and Figure 6.12a. Material properties and thicknesses for the calculations are shown in Table 6.1.

Table 6.1. Material properties and thicknesses

	Young's modulus (GPa)	Poisson's ratio	$d_{31} = d_{32}$ (m/V)	t (mm)
IPMC	1.158*	0.487	1.750×10^{-7}	0.3
Plastic film	0.1	0.3	N/A	0.1

Pt (~6%) heavy IPMC

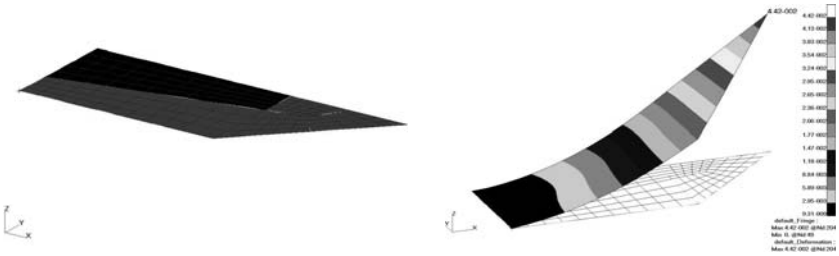

(a) Finite-element model (b) Deformed shape

Figure 6.11. Flapping simulation for flapping wing #1 ([27])

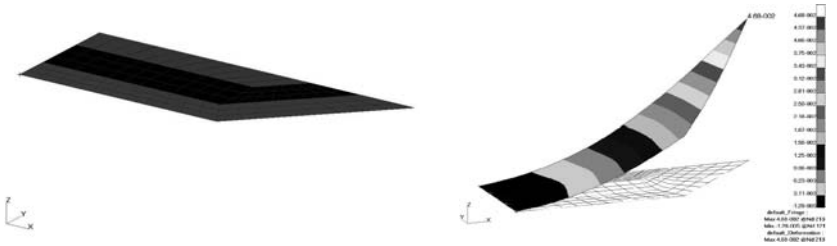

(a) Finite-element model (b) Deformed shape

Figure 6.12. Flapping simulation for flapping wing #2 ([27])

The flap-up displacement and twisting angle at the tip under 3 V (*i.e.*, $E_3 = 10$ V/mm) are calculated as 4.42 cm and 3.4º, for Wing #1, and 4.68 cm and 9.1º, for Wing #2. The deformed shapes are shown in Figure 6.11b and Figure 6.12b for Wing #1 and #2, respectively. Wing #2 is the better design for the flapping wing in terms of a twisting angle. Noted that our analysis is based on linear elasticity and thus may not accurately predict the actuation displacement. However, the present approach provides a simple but effective design tool to determine the shape of an IPMC actuator for a specific purpose.

6.6 Summary and Acknowledgments

In this chapter, the fundamental properties and a brief summary of recent progress in ionic polymeric-metal composites (IPMCs) as smart biomimetic sensors, actuators, and artificial muscles were presented. In the following Chapters 7, 8, 9, and 10, detailed robotics-related work on IPMCs is presented by many investigators from RIKEN, AIST, the Tokyo Institute of Technology, Tohoku University, the University of Nevada, Las Vegas, and the University of Nevada, Reno.

Also, I would like to extend my special thanks to many earlier investigators including Drs. K. Oguro (Osaka National Research Institute), M. Shahinpoor (University of New Mexico), K. Asaka (Research Institute for Cell Engineering, AIST), Y. Bar-Cohen (NASA Jet Propulsion Laboratory), S. Nemat-Nasser (University of California, San Diego), and D. Leo (Virginia Tech). Their dedicated work toward IPMCs is invaluable. The research work regarding IPMCs performed by Drs. H.C. Park, S.K. Lee, I.S. Park and, Mr. D. Kim is also appreciated.

6.7 References

[1] K.J. Kim, W. Yim, J.W. Paquette, and D. Kim, Ionic Polymer-Metal Composites for Underwater Operation, Journal of Intelligent Materials Systems and Structures (JIMSS), (2006, in print).

[2] D. Kim and K.J. Kim, Experimental Investigation on Electrochemical Properties of Ionic Polymer-Metal Composite, Journal of Intelligent Materials Systems and Structures (JIMSS), (2006, in print).

[3] D.Y. Lee, M.-H. Lee, K.J. Kim, S. Heo, B.-Y. Kim, and S.-J. Lee, Effect of Multiwalled Carbon Nanotube (M-CNT) Loading on M-CNT Distribution Behavior and the Related Electromechancial Properties of the M-CNT Dispersed Ionomeric Nanocomposites, Surface Coatings and Technology, Vol. 200(5-6), pp. 1916-192 (2005).

[4] S-K. Lee, H.C. Park, and K.J. Kim, Equivalent Modeling for Ionic Polymer-Metal Composite Actuators Based on Beam Theories, Smart Materials and Structures, Vol. 14, pp. 1363-1368 (2005).

[5] J.W. Paquette, K.J. Kim, D. Kim, and W. Yim, The Behavior of Ionic Polymer-Metal Composites in a Multi-Layer Configuration, Smart Materials and Structures, Vol. 14, 881-888 (2005).

[6] M. Shahinpoor and K.J. Kim, Ionic Polymer-Metal Composite-IV: Industrial and Mechanical Applications, Smart Materials and Structures, Vol. 14, 197-214 (2005); M. Shahinpoor and K.J. Kim, Ionic Polymer-Metal Composites: III. Modeling and Simulation as Biomimetic Sensors, Actuators, Transducers, and Artificial Muscles, Smart Materials and Structures, Vol. 13, pp. 1362-1388 (2004); K.J. Kim and M. Shahinpoor, Ionic Polymer-Metal Composites - II. Manufacturing Techniques, Smart Materials and Structures, Vol. 12, No. 1, pp. 65-79 (2003); M. Shahinpoor and K.J. Kim, Ionic Polymer-Metal Composites – I. Fundamentals, Smart Materials and Structures, Vol. 10, pp. 819-833 (2001).

[7] J.-D. Nam, J.H. Lee, J.H. Lee, H. Choe, K.J. Kim, and Y.S. Tak, Water Uptake and Migration Effects of Electroactive IPMC(Ion-Exchange Polymer-Metal Composite) Actuator, Sensors and Actuators A: Physical, Vol. 118, pp. 98-106 (2005).

[8] J.W. Paquette, K.J. Kim, and D. Kim, Low Temperature Characteristics of Ionic Polymer-Metal Composite Actuators, Sensors and Actuators A: Physical, Vol. 118, pp. 135-143 (2005).
[9] J. Paquette and K.J. Kim, Ionomeric Electro-Active Polymer Artificial Muscle for Naval Applications, IEEE Journal of Oceanic Engineering (JOE), Vol. 29, No. 3, pp. 729-737 (2004).
[10] J. Paquette, K.J. Kim, J.-D. Nam, and Y. S. Tak, An Equivalent Circuit Model for Ionic Polymer-Metal Composites and Their Performance Improvement by a Clay-Based Polymer Nano-Composite Technique, Journal of Intelligent Materials Systems and Structures (JIMSS), Vol. 14, pp. 633-642 (2003).
[11] J.-D. Nam, H.R. Choi, Y.S. Tak, and K.J. Kim, Novel Electroactive, Silicate Nanocomposites Prepared to Be Used as Actuators and Artificial Muscles, Sensors and Actuators: A. Physical, Vol. 105, pp. 83-90 (2003).
[12] M. Shahinpoor, K.J. Kim, and D. Leo, Ionic Polymer-Metal Composites as Multifunctional Materials, Polymer Composites, Vol. 24, No. 1, pp. 24-33 (2003).
[13] M. Shahinpoor and K.J. Kim, Experimental Study of Ionic Polymer-Metal Composites in Various Cation Forms: Actuation Behavior, Science and Engineering of Composite Materials, Vol. 10, No. 6, pp. 423-436 (2002).
[14] M. Shahinpoor and K.J. Kim, Mass Transfer Induced Hydraulic Actuation in Ionic Polymer-Metal Composites, Journal of Intelligent Materials Systems and Structures (JIMSS), Vol. 13, No. 6, pp. 369-376 (2002).
[15] M. Shahinpoor and K.J. Kim, A Novel Physically-Loaded and Interlocked Electrode Developed for Ionic Polymer-Metal Composites (IPMCs), Sensors and Actuator: A. Physical, Vol. 96, No. 2/3, pp. 125-132 (2002).
[16] K.J. Kim and M. Shahinpoor, Development of Three Dimensional Ionic Polymer-Metal Composites as Artificial Muscles, Polymer, Vol. 43(3), pp. 797-802 (2002).
[17] M. Shahinpoor and K.J. Kim, The Effect of Surface-Electrode Resistance on the Performance of Ionic Polymer-Metal Composite (IPMC) Artificial Muscles, Smart Materials and Structures, Vol. 9, No. 4, pp. 543-551 (2000).
[18] P.G. de Gennes, K. Okumura, M. Shahinpoor, and K.J. Kim, Mechanoelectric Effects in Ionic Gels, Europhysics Letters, Vol. 50, No. 4, pp. 513-518 (2000).
[19] S. Nemat-Nasser, Micromechanics of Actuation of Ionic Polymer-Metal Composites, Journal of Applied Physics, Vol. 92, No. 5, pp. 2899-2910 (2002).
[20] S. Nemat-Nasser and C.W. Thomas, Ionomeric Polymer-Metal Composites, in Electroactive Polymer (EAP) Actuators as Artificial Muscles, Reality, Potential, and Challenges, ed. Bar-Cohen, Y., SPIE Press, Washington, (2001).
[21] K. Oguro, K. Asaka, and H. Takenaka, Actuator Element, U.S. Patent #5,268,082, (1993).
[22] S. Tadokoro, T. Takamori, T., and K. Oguro, Modeling IPMC for Design of Actuation Mechanisms, in Electroactive Polymer (EAP) Actuators as Artificial Muscles, Reality, Potential, and Challenges, ed. Bar-Cohen, Y., SPIE Press, Washington, U.S.A., (2001).
[23] K. Asaka, K. Oguro, Y. Nishimura, M. Mizuhata, and H. Takenaka, Bending of Polyelectrolyte Membrane-Platinum Composites by Electric Stimuli, I. Response Characteristics to Various Waveforms, Polymer Journal, Vol. 27, No. 4, pp. 436-440 (1995).
[24] B.J. Akle, M.D. Bennet, and D. Leo, High Strain Ionomeric-Ionic Liquid Electroactive Actuators Sensors and Actuators A (in press, 2006).
[25] M.D. Bennett and D.J. Leo, Ionic Liquids as Solvents for Ionic Polymer Transducers, Sensors and Actuators A: Physical, Vol. 115. pp. 79–90 (2004).
[26] D.E. Alexander, Nature's Flyers, Chapter 4. London, The Johns Hopkins University Press (2003).

[27] H.C. Park, S. Lee, and K.J. Kim, Equivalent Modeling for Shape Design of IPMC (Ionic Polymer-Metal Composite) as Flapping Actuator, Key Engineering Materials, Vol. 297-300, pp. 616-621 (2005).